PHYSICAL REVIEW A **79**, 030303(R) (2009)

All-optical-fiber polarization-based quantum logic gate

Alex S. Clark,[1] Jérémie Fulconis,[1] John G. Rarity,[1] William J. Wadsworth,[2] and Jeremy L. O'Brien[1,*]
[1]*Centre for Quantum Photonics, H. H. Wills Physics Laboratory and Department of Electrical and Electronic Engineering, University of Bristol, Merchant Venturers Building, Woodland Road, Bristol BS8 1UB, United Kingdom*
[2]*Centre for Photonics and Photonic Materials, Department of Physics, University of Bath, Claverton Down, Bath BA2 7AY, United Kingdom*

(Received 8 October 2008; revised manuscript received 15 January 2009; published 26 March 2009)

We report an experimental demonstration of a quantum controlled-NOT gate constructed entirely in optical fiber and operating on polarization-encoded single-photon qubits. We operated this gate using two heralded optical fiber single-photon sources and found an average logical fidelity of 90% and an average process fidelity of $0.83 \leq \bar{F} \leq 0.91$. On the basis of a simple model we are able to conclude that imperfections are primarily due to the photon sources, meaning that the gate itself works with very high fidelity. Such all fiber quantum information processing will likely have important applications in future quantum networks.

DOI: 10.1103/PhysRevA.79.030303 PACS number(s): 03.67.Lx, 42.50.Ex, 42.81.−i

Anticipated technologies that harness uniquely quantum-mechanical effects [1] include quantum computing, quantum lithography, and quantum metrology. However, the only quantum technology in existence today is quantum cryptography [2,3], where an attempt to measure information encoded in the state of a photon results in a detectable disturbance. More sophisticated quantum networks will require multiple nodes with the ability to implement small-scale quantum processing [4–6]. Such networks will rely on optical fiber links, making fiber-based photon generation and information processing of key technological importance. Here we demonstrate both elements in an all-fiber realization of a controlled-NOT (CNOT) gate using two heralded photonic crystal fiber (PCF) single-photon sources. We measure an average logical fidelity of 90% and an average process fidelity of $0.83 \leq \bar{F} \leq 0.91$. Using a simple model we find the remaining discrepancy to be due almost entirely to spectral properties of the photon sources, demonstrating near-perfect operation of the fiber CNOT gate itself.

Single photons are unique among the handful of quantum systems being explored for quantum technologies for their extremely low decoherence and low-loss high-speed propagation properties. They are the logical choice for quantum metrology [7,8] and lithography [9], are a leading approach to quantum information processing [10], and appear to be indispensable for quantum communication [2,3]. Quantum communication systems based on optical fiber "plug-and-play" devices are now commercially available from several companies. These systems are currently limited in the number of users and rely on weak laser pulses to approximate single photons. Key steps toward future quantum networks with multiple secure links are to use single-photon sources and introduce entangling capabilities. Such networks will likely consist of fiber links with small-scale quantum processing at individual nodes, with the ability to generate and measure entanglement. The CNOT gate is the canonical quantum logic element capable of performing all of these tasks and will likely play an important role in quantum networks, where its applications include entanglement generation, state discrimination [11], parity encoding [12], Bell state measurements [13], and entanglement purification [14].

A CNOT gate operating on the polarization state of two photons [15,16] is shown schematically in Fig. 1(a). The gate has two classical interferometers and one quantum interfer-

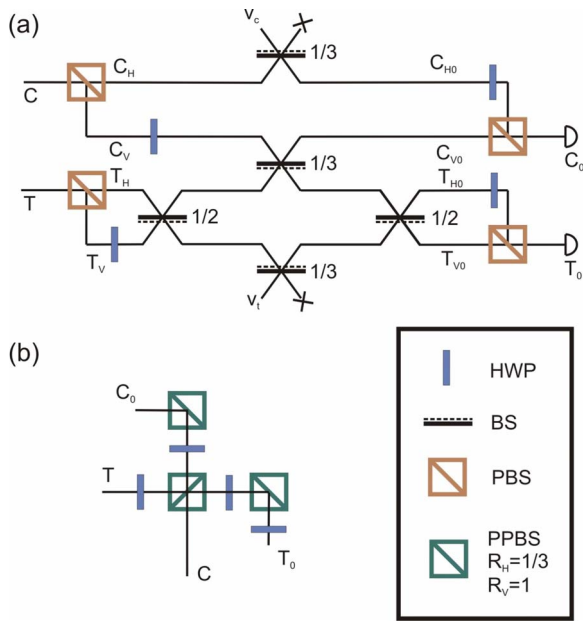

FIG. 1. (Color online) A two-photon quantum CNOT gate. (a) The setup involves conversion from polarization encoding to spatial mode encoding via the use of polarizing beamsplitters (PBSs) in the control c and target t optical modes, and half wave plates (HWPs) to make all polarizations the same, followed by a nonclassical interference at the central beamsplitter (BS) with a reflectivity equal to 1/3. The other two 1/3 beamsplitters serve to adjust the output amplitudes while 1/2 beamsplitters perform Hadamard operations on the target mode. The dotted lines indicates a phase shift on reflection [15]. The beams are then recombined at polarizing beamsplitters, creating two interferometers. Success of the gate is conditional upon detecting a photon at each of the target and control outputs, which occurs with probability of 1/9. (b) The PPBS simplification of the gate.

*Jeremy.OBrien@bristol.ac.uk

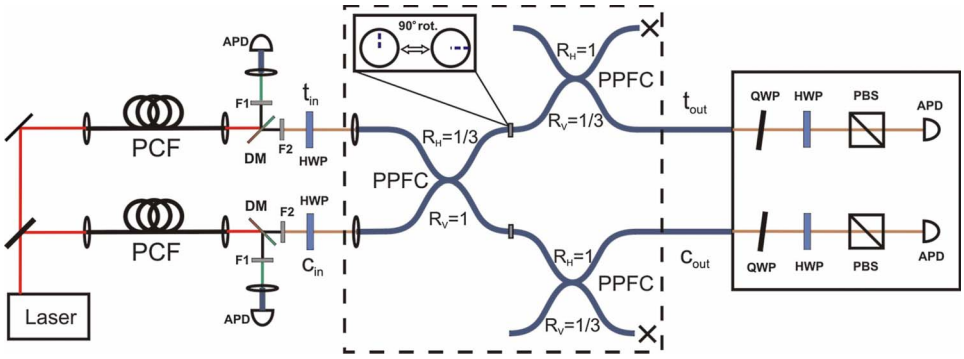

FIG. 2. (Color online) An all-optical fiber quantum CNOT gate operated with heralded photonic crystal fiber single-photon sources. A ps 708 nm Ti:sapphire laser pumps two PCFs creating a nondegenerate pair of photons at 583 and 900 nm. These are separated at dichroic mirrors (DMs) and pass through interference filters F1 and F2 with bandwidths of 0.2 and 0.8 nm, respectively. Detection of the 583 nm photons heralds the arrival of the 900 nm control c and target t photons at the inputs to the CNOT gate. HWPs are used to create logical and diagonal input states. The gate consists of three PPFCs with the reflectivities for horizontal and vertical photons as shown. The polarizations of the idler photons are then analyzed using a HWP and a PBS cube for each arm. Note that the Hadamard operations before and after the gate are integrated into the encoding and analysis wave plates. Also inserted here are quarter-wave plates (QWPs) which may be tilted to correct for any phase accumulated through the gate. All four photons are then detected using Perkin Elmer silicon avalanche photodiodes (APDs) and sent to an electronic fourfold coincidence counting circuit for analysis.

ometer. The original demonstration of this circuit relied on a sophisticated bulk-optics implementation to maintain a stable phase in converting between polarization and path encoding [17,18]. Such interferometric tricks are not possible in optical fibers, making a fiber version of this CNOT gate technologically challenging. This classical interference requirement was circumvented in demonstrations that used "partially polarizing beamsplitters" (PPBSs) with different reflectivities for each polarization: $R_H=1/3$ and $R_V=1$ for horizontally and vertically polarized photons, respectively [Fig. 1(b)] [19–21], including one at telecommunications wavelengths [22]. Rather than separating the two polarizations to enable different operations on each, these gates use optical elements that perform different operations on the two polarizations. Whether such an approach would work for optical fibers, enabling the realization of an all-fiber CNOT gate, was previously an open question.

We used the network of three partially polarizing fiber couplers (PPFCs) and the two heralded PCF single-photon sources [23], shown schematically in Fig. 2, to implement an all-fiber CNOT gate. The PPFCs were fabricated from two polarization-maintaining fibers that are polished to the core, coated with metal and dielectric films then fused together, such that the coupling for the H mode on the slow axis is supported but the V mode (fast axis) is denied coupling. This results in a polarization-maintaining fiber coupler with reflectivities $R_H=1/3$ and $R_V=1$.

The first PPFC in Fig. 2 enables the control c and target t photons to interact via quantum interference and subsequent photon detection [24]. The other two PPFCs serve to balance the quantum amplitudes and thereby maintain a uniform success probability of 1/9 and require a 90° rotation with respect to the first PPFC to effectively swap the reflectivities to $R_H=1$ and $R_V=1/3$. The circuit retains the polarization encoding throughout, removing the need for classical interference, while the PCF sources signal the arrival of the control and target photons, which are spectrally filtered to ensure high-visibility quantum interference. This fiber configuration guarantees excellent spatial mode matching required to realize high-fidelity quantum interference, allows the gate to be miniaturized, and exhibits the criteria for scalable and integrable photonic quantum circuits.

Polarization-maintaining fibers allow two orthogonal polarizations (those parallel to the axes of birefringence) to propagate without rotation (horizontal and vertical in our case). These two polarizations travel at a different speed through the fiber, such that a superposition state will be rotated and ultimately decohere. This is coarsely corrected for within the gate by the 90° rotation at the connections between PPFCs (Fig. 2). The remaining phase shift is corrected by a tilted birefringent wave plate at each output of the gate.

Following the method proposed in [25] and implemented in [21], we measure truth tables for two complementary bases. We choose the computational (ZZ) basis $\{|0\rangle=|V\rangle, |1\rangle=|H\rangle\}$ and the diagonal (XX) basis $\{|0\rangle=(|H\rangle+|V\rangle)/\sqrt{2}, |1\rangle=(|H\rangle-|V\rangle)/\sqrt{2}\}$. The 16 element truth tables are defined as the probability of obtaining each of the four logical output states for each logical input. The results are shown in Fig. 3. From these data we calculate average logical fidelities $F_{ZZ}=0.90\pm0.02$ for the computational (ZZ) basis and $F_{XX}=0.89\pm0.02$ for the diagonal (XX) basis. These two classical fidelities can be used to place bounds on the quantum process fidelity F_P [25],

$$F_{XX}+F_{ZZ}-1\leq F_P\leq \min\{F_{XX},F_{ZZ}\} \tag{1}$$

which gives $0.79\leq F_P\leq 0.89$ for our all-fiber gate. This corresponds to an average process fidelity [18,26] of $0.83\leq \bar{F}\leq 0.91$.

The quantum interference visibility V at the central PPFC is 94%, after correction for multiphoton emission, most likely due to spectral mismatch of the photons [23]. To understand and quantify the effect of this error we have developed a model based on [15] which also includes imperfect

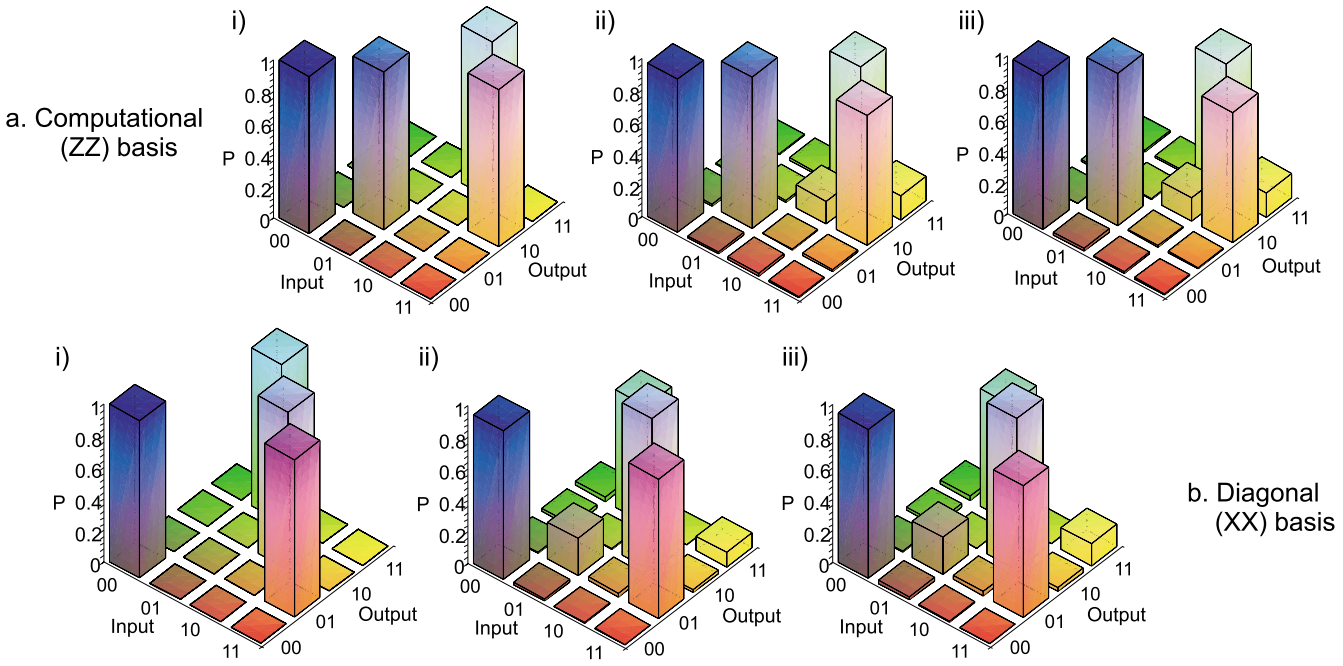

FIG. 3. (Color online) Truth table results for the gate operating in two orthogonal bases: (a) the computational (*ZZ*) basis and (b) the diagonal (*XX*) basis. We show (i) the ideal operation, (ii) the experimental data, and (iii) the results from the model.

state preparation and analysis (Fig. 4). The mode mismatch is modeled by introduction of two extra spatial modes C_{H2} and C_{V2}; although this is modeled as spatial, mismatch in all degrees of freedom is equivalent [27]. The beamsplitter values in the model are determined directly from measurement of the PPFC reflectivities. Incorrect state preparation and analysis is modeled using beamsplitters which mix the target and control *H* and *V* modes. Ideal operation in the computational basis corresponds to $\eta_{3a}=\eta_{4a}=1$ and $\eta_{3b}=\eta_{4b}=1/2$, and in the diagonal basis $\eta_{3a}=\eta_{4a}=1/2$ and $\eta_{3b}=\eta_{4b}=1$ (i.e., control and target are swapped). Imperfect quantum interference results in (equal) error terms on the diagonal of the truth table for the control "1" inputs in both bases. Truth tables from the full model are shown in Fig. 3.

As it is not possible to use the average fidelity to measure the distance between two nonideal truth tables, we introduce

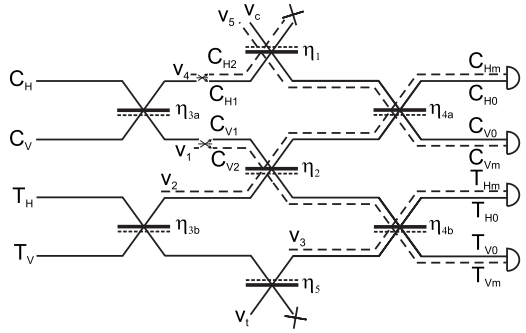

FIG. 4. A model for CNOT gate operation. The additional modes (dashed lines) are used to model mode mismatch at the central beamsplitter. The beamsplitters are given reflectivities η_i. The dotted-line side of the beamsplitters indicates the side at which a π phase shift occurs upon the incident photon.

the similarity *S* to compare the truth table generated by the model *M* and that measured experimentally *E*,

$$S=\left(\sum_{i,j=1}^{4}\sqrt{M_{i,j}E_{i,j}}\right)^2\Big/16 \qquad (2)$$

which is a generalization of the average fidelity based on the (classical) fidelity between probability distributions [28,29].

The similarity to the model is shown in Table I for three different cases: ideal operation, the case where only imperfect quantum interference is included, and the case where imperfect encoding and decoding are also incorporated. The small deviations of the beamsplitter values from the perfect 1/3 case proved to have a negligible difference on the fidelity, but were retained for completeness. The results show that while there were some small errors introduced through the wave-plate positioning, most of the errors, 7.9% and 7.7% for the computational and diagonal bases, respectively, were due to an imperfect interference visibility. The source of mode mismatch is unlikely to be spatial, as it has been shown previously that fiber beamsplitters exhibit interference visibilities of greater than 99% [30]. It is more likely that the

TABLE I. Similarity between the model and experimental results for the ideal gate, the case with imperfect visibility of the quantum interference, and the full model including imperfect visibility and imperfect state preparation and analysis.

Model type	S_{ZZ}	S_{XX}
Ideal	0.895	0.883
Interference	0.974	0.960
Full model	0.997	0.998

mismatch arises through spectral differences between the photons emitted from the separate sources [23]. Introducing imperfect state preparation and analysis causes the similarity of the model with the experimental results to rise by a further 2.3% and 3.8%, reaching 99.7% and 99.8% for the computational and diagonal bases, respectively, confirming near-perfect operation of the CNOT gate itself.

Part of the great promise of quantum technologies has already been delivered through the development of commercial quantum cryptography systems. However, it is widely anticipated that more advanced quantum networks can be built on the same underlying principles of quantum-enhanced security. An essential component will be the ability to generate and process photonic quantum information all in fiber. While a recent demonstration of quantum circuits in waveguides [31,32] is promising for optical quantum computing, the high-fidelity fiber CNOT gate operating with fiber single-photon sources demonstrated here shows that it is possible to implement all-fiber quantum logic, which is more suitable for quantum networks. For example, all three components—photon generation, encoding, and decoding—used in a recent demonstration of entanglement distribution over a fiber communication channel using a decoherence-free subspace [13] could all now be implemented in optical fiber. All-fiber quantum information processing has many further important applications in quantum communication [11–14] and may also find applications in less mature quantum technologies, such as computing, lithography, and metrology, as well as in the fundamental science of quantum optics, where optical circuits are reaching the technical limits of what is possible with bulk optics (e.g., [33,34]).

W.J.W. is supported by the Royal Society. J.G.R. is supported by the Royal Society and the Wolfson Foundation. This work was supported by the UK EPSRC, QIP IRC, 1-phot, the U.S. IARPA, and QAP.

[1] M. A. Nielsen and I. L. Chuang, *Quantum Computation and Quantum Information* (Cambridge University Press, Cambridge, England, 2000).
[2] N. Gisin and R. Thew, Nat. Photonics **1**, 165 (2007).
[3] N. Gisin, G. Ribordy, W. Tittel, and H. Zbinden, Rev. Mod. Phys. **74**, 145 (2002).
[4] L.-M. Duan, M. D. Lukin, J. I. Cirac, and P. Zoller, Nature (London) **414**, 413 (2001).
[5] H.-J. Briegel, W. Dür, J. I. Cirac, and P. Zoller, Phys. Rev. Lett. **81**, 5932 (1998).
[6] O. Ahonen, M. Möttönen, and J. L. O'Brien, Phys. Rev. A **78**, 032314 (2008).
[7] T. Nagata, R. Okamoto, J. L. O'Brien, K. Sasaki, and S. Takeuchi, Science **316**, 726 (2007).
[8] B. L. Higgins, D. W. Berry, S. D. Bartlett, H. M. Wiseman, and G. J. Pryde, Nature (London) **450**, 393 (2007).
[9] M. D'Angelo, M. V. Chekhova, and Y. Shih, Phys. Rev. Lett. **87**, 013602 (2001).
[10] J. L. O'Brien, Science **318**, 1567 (2007).
[11] G. J. Pryde, J. L. O'Brien, A. G. White, and S. D. Bartlett, Phys. Rev. Lett. **94**, 220406 (2005).
[12] J. L. O'Brien, G. J. Pryde, A. G. White, and T. C. Ralph, Phys. Rev. A **71**, 060303(R) (2005).
[13] T. Yamamoto, K. Hayashi, S. K. Ozdemir, M. Koashi, and N. Imoto, Nat. Photonics **2**, 488 (2008).
[14] J.-W. Pan, S. Gasparoni, R. Ursin, G. Weihs, and A. Zeilinger, Nature (London) **423**, 417 (2003).
[15] T. C. Ralph, N. K. Langford, T. B. Bell, and A. G. White, Phys. Rev. A **65**, 062324 (2002).
[16] H. F. Hofmann and S. Takeuchi, Phys. Rev. A **66**, 024308 (2002).
[17] J. L. O'Brien, G. J. Pryde, A. G. White, T. C. Ralph, and D. Branning, Nature (London) **426**, 264 (2003).
[18] J. L. O'Brien, G. J. Pryde, A. Gilchrist, D. F. V. James, N. K. Langford, T. C. Ralph, and A. G. White, Phys. Rev. Lett. **93**, 080502 (2004).
[19] N. K. Langford, T. J. Weinhold, R. Prevedel, K. J. Resch, A. Gilchrist, J. L. O'Brien, G. J. Pryde, and A. G. White, Phys. Rev. Lett. **95**, 210504 (2005).
[20] N. Kiesel, C. Schmid, U. Weber, R. Ursin, and H. Weinfurter, Phys. Rev. Lett. **95**, 210505 (2005).
[21] R. Okamoto, H. F. Hofmann, S. Takeuchi, and K. Sasaki, Phys. Rev. Lett. **95**, 210506 (2005).
[22] J. Chen, J. B. Altepeter, M. Medic, K. F. Lee, B. Gokden, R. H. Hadfield, S. W. Nam, and P. Kumar, Phys. Rev. Lett. **100**, 133603 (2008).
[23] J. Fulconis, O. Alibart, J. L. O'Brien, W. J. Wadsworth, and J. G. Rarity, Phys. Rev. Lett. **99**, 120501 (2007).
[24] E. Knill, R. Laflamme, and G. J. Milburn, Nature (London) **409**, 46 (2001).
[25] H. F. Hofmann, Phys. Rev. Lett. **94**, 160504 (2005).
[26] A. Gilchrist, N. K. Langford, and M. A. Nielsen, Phys. Rev. A **71**, 062310 (2005).
[27] P. P. Rohde, G. J. Pryde, J. L. O'Brien, and T. C. Ralph, Phys. Rev. A **72**, 032306 (2005).
[28] G. J. Pryde, J. L. O'Brien, A. G. White, S. D. Bartlett, and T. C. Ralph, Phys. Rev. Lett. **92**, 190402 (2004).
[29] T. C. Ralph, S. D. Bartlett, J. L. O'Brien, G. J. Pryde, and H. M. Wiseman, Phys. Rev. A **73**, 012113 (2006).
[30] T. B. Pittman and J. D. Franson, Phys. Rev. Lett. **90**, 240401 (2003).
[31] A. Politi, M. J. Cryan, J. G. Rarity, S. Yu, and J. L. O'Brien, Science **320**, 646 (2008).
[32] G. D. Marshall, A. Politi, J. C. F. Matthews, P. Dekker, M. Ams, M. Withford, and J. L. O'Brien, e-print arXiv:0902.4357.
[33] R. Okamoto, J. L. O'Brien, H. F. Hofmann, T. Nagata, K. Sasaki, and S. Takeuchi, Science **323**, 483 (2009).
[34] B. P. Lanyon, M. Barbieri, M. P. Almeida, T. Jennewein, T. C. Ralph, K. J. Resch, G. J. Pryde, J. L. O'Brien, A. Gilchrist, and A. G. White, Nat. Phys. **5**, 134 (2009).